Journal of Solid Mechanics Vol. 14, No. 2 (2022) pp. 131-146
DOI: 10.22034/jsm.2020.1908867.1641

Multi-Objective Optimization of Shot-Peening Parameters Using Modified Taguchi Technique

M. Hassanzadeh , S.E. Moussavi Torshizi *

Faculty of Mechanical and Energy Engineering, Shahid Beheshti University, Tehran, Iran

Received 1 February 2022; accepted 27 March 2022

ABSTRACT

Shot-peening is a surface treatments utilized extensively in the industry to enhance the performance of metal parts against fatigue. This paper aimed to find the optimal parameters of the shot-peening process based on the finite elements model and the Taguchi method. The effects of three peening parameters (shot diameter, shot velocity, coverage percentage) are investigated on residual stress and roughness using Taguchi method. A new Taguchi technique is proposed by combining it with desirability function to optimize the shot-peening parameters that simultaneously provide two or more responses in an optimal mode. The results show that the coverage percentage has the most influence on the surface stress and maximum compressive stress whereas the velocity and diameter of the shot are the most effective parameters on the depth of compression stress. The shot velocity is the main factor of the surface roughness due to the shot peening. Through the proposed structure, optimal conditions can be obtained for surface stress and roughness simultaneously with high-coverage and low-velocity. Eventually, results reveal the effectiveness of the proposed strategy in stand point of saving time and cost.

Keywords : Shot peening; Taguchi method; Desirability function; Residual stresses; Roughness.

1 INTRODUCTION

SHOT-PEENING is frequently considered as an effective approach in enhancing the behavior of the mechanical components against fatigue [1-3]. One can attribute the advantageous effects of the process to the surface hardening and the residual stresses field [2, 3]. The results of shot-peening are dependent on the mechanical features of the desired material and the circumstances of the process (shot type, shot velocity, coverage, impact angle, etc.). When the parameters of shot-peening are not chosen properly, one can see adverse effects on fatigue resistance [2, 3]. This issue demonstrates that the selection of shot-peening parameters is important to increase the fatigue life. Therefore, it is critical to estimate the effect of the shot-peening parameters on fatigue life and to select it optimally and appropriately. Numerical, analytical, and experimental approaches can be applied to estimate the shot-peening effects [4, 5]. The applied analytical approach was encountered with restrictions; therefore, numerous empirical researches have been performed on the shot-peening field [6, 7]. In comparison with the experimental test,

*Corresponding author.
E-mail address: e_moussavi@sbu.ac.ir (S.E. Moussavi Torshizi)

numerical simulation can be used to reduce time and costs, which can be, mentioned single-shot [8, 9] or multi-shot simulation. [10, 11]. Recently the fully randomized scattering of shots, similar to the shot-peening in a real model in comparison with uniformly distributed models of shots, a number of models are established by Ghasemi et al. [12], Miao et al. [13], and Mahmoudi et al. [14]. In addition to modeling shot-peening, its optimal parameters have been studied by researchers. Nam et al. [15] and AlSumait [16] have determined the optimal coverage of the maximum fatigue life. Petit-Renaud et al. [17] and Romero et al. [18] optimized the maximum compressive stress in the form of an objective function. Vielma et al. [19] and Unal [20] considered roughness as an objective function. Bhuvaraghan et al. [21] investigated multi-objective shot-peening through genetic algorithm approach and optimized the compressive residual stress when considering work hardening and roughness under certain limits. Baragetti [22] optimized the maximum compressive stresses and the surface roughness, the compressive residual stress depth and the maximum compressive stress depth, simultaneously. Seddik et al. [23] have managed to optimize two objective functions of damage variable and compressive residual stress for the shot-peening process. The Taguchi method is an efficient approach to reduce the number of experiments and save time and cost [24]. In this method, the appropriate levels for each process parameter must be identified and a standard orthogonal array is selected accordingly. Using Taguchi's approach, George et al. [25] optimized the shot-peening intensity. Khani et al. [26] obtained the optimal parameter of the shot-peening process for the low carbon steel by Taguchi's technique. In [27] Taguchi method is used to analysis shot peening effects on grain size, hardness, and residual stress. In all of the above-mentioned research, the objective functions were examined separately and single. Taguchi method is highly efficient and fast which gives effective parameters and optimal level. However, in this approach, the objective functions must be single-objective. A little attention has paid to multiple responses optimization using Taguchi method. Several methods have been tested in Taguchi method for multiple response problems. To unify the objectives, a transformation of a multi-response design into a single response one has been done based on mathematical techniques. Shiau [28] proposed a method in which a weight has been allotted to the S/N ratios of each quality responses. Then, by using the combined S/N ratios, the optimal factor levels, have been achieved. In [29], Tong et al. utilized the weighted normalized quality loss summation of responses; it is used to calculate optimal factor levels. However, it remains difficult to define a weight for each response. Using a tentative approach, in Logothetis and Haigh [30] and Pignatello [31] works, the optimal factor levels are determined using regression techniques which leads to an increase in the complexity of computational process. In [32], Tong and Su employed a method, in which the fuzzy set theory is used for optimization of response production process. In Fuzzy multiple attribute decision-making, we encounter selection between among some choices, that each of them, has multiple conflicting attributions to the others. Nevertheless, this method will not be able to reach to solve multiple response problems, because it requires incorporating the knowledge of experts into the formula. By using principal component analysis method, (PCA), Su and Tong [33] and Antony [34], performed the transformation of multiple responses problem into a few uncoupled responses one, which used to solve multi-response problem. However, the mentioned method, (PCA) has its deficiency. firstly, how to compromise on choose feasible solution when multiple principal components of an eigenvalue, which is greater than one, are unknown and, the secondly the performance index of multi-responses has fewer superiority compared to the original response variables, if the selected principal components have less variation than can be introduced by total variation. In [35], Liao and Chen used the data envelopment analysis (DEA) on the basis of ranking approach, to determine optimal factor levels in Taguchi method for multiple response problem. The majority of traditional DEA schemes, have complete flexibility of weight which probably, results in unrealistic weighting for detection and decision making unit which is a basic disadvantage among them [36, 37]. In this paper, we proposed a simple, but effective method to solve multiple response using Taguchi-method.

In this study, the Taguchi technique is combined with the desirability function to eliminate the defect of the conventional Taguchi method and it can be used for multi-objective optimization. The new approach is employed to multi-objective optimizing the shot-peening parameters. The study addresses the influence of shot-peening factors on surface stress, maximum compressive stress, the depth of the maximum compressive stress, depth of compressive stress layer and roughness Ra of plate made of AISI 420 steel.

2 FINITE ELEMENT MODEL

Finite Element Method (FEM) is one of the prevalent method to determine the displacements, stresses and other quantities. The simulation of shot-peening was done using the commercial code ABAQUS 2017. The explicit solver (explicit) was employed to analyze the dynamic effects of shot-peening. In order to create a model with specific inputs (shot-peening conditions, material, type of the shots and so on) the code was written based on the Python script. FEM analysis was developed using a damping coefficient [38] not only to decrease stress oscillations, but also to avoid uncontrolled oscillations after collisions in the simulation. The material damping is:

$$D = \alpha M + \beta K \tag{1}$$

In the above equation, D, M, and K are damping, mass and stiffness matrices, respectively. The effective damping was considered by a stiffness proportional damping coefficient $\beta = 2\times10^{-9}\,s$. The following methodology was employed for obtaining mass proportional damping (α). The minimum modal frequency ω_0 is estimated as:

$$\omega_0 = \frac{1}{H}\sqrt{\frac{2E}{\rho}} \tag{2}$$

where E is the Young's modulus, ρ is density and H is the thickness of the body. The mass proportional damping is calculated as:

$$\alpha = 2\omega_0\xi \tag{3}$$

where ξ is the modal damping parameter. To decay the unwanted low-frequency oscillations [39], ξ was equal to 0.5. Thermal and spring-back effects are neglected because of the negligible impact on the results. The proposed 3D model predicts residual compressive stress, plastic deformation and surface integrity.

2.1 Boundary condition and geometry

For reducing the effect of boundary conditions of the body edges, the body was modeled with dimensions of $6D \times 6D \times h$, where D is the diameter of the shot and h is the target thickness. The only central area with dimensions of $2D \times 2D$ in upper surface was encountered with multiple shots as is seen in Fig. 1. Eight-node linear solid elements with reduced integration C3D8R was chosen to mesh the body. For the accuracy and efficiency of the results, a fine-mesh grid arrangement 0.02 *mm* × 0.02 *mm* × 0.02 *mm* for the shot peened area and a greater mesh size was considered for the rest of the body. General contact (Explicit) was used for the contact. All the target surfaces except the upper surface were fixed. The size of the model was considered large enough with respect to the size of the shot to eliminate the effects of the boundary condition. Without applying the constraint in the vertical direction, similar results would be achieved. The initial velocity applied to the shots perpendicular to the upper surface of the body (y-axis) and were fixed in the other directions.

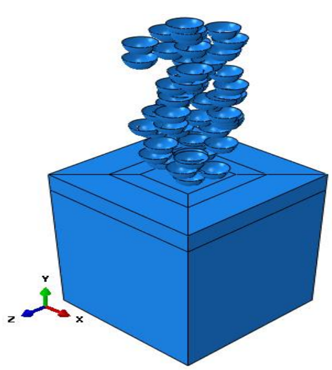

Fig.1
Three-dimensional finite element model of shot-peening.

2.2 Material model

The target material was AISI420 martensitic stainless steel and Johnson-Cook model is considered to simulate this material (Eq. (4)).

$$\sigma=\left(A+B(\varepsilon^{p})^{n}\right)\left(1+C\log\left(\frac{\dot{\varepsilon}^{p}}{\dot{\varepsilon}_{0}}\right)\right)\left(1-\left(\frac{T-T_{r}}{T_{m}-T_{r}}\right)^{m}\right) \tag{4}$$

where *A, B, C, n* and *m* are the constants of the material. The parameters ε^p is the equivalent plastic strain, $\dot{\varepsilon}^p$ is the plastic strain rate, $\dot{\varepsilon}_0$ is the reference strain rate, T_r is the room temperature, T_m is the melting temperature and T is the reference temperature. Johnson Cook's parameters and other material parameters for AISI420 are presented in Tables 1 and 2. The shots were considered rigid.

Table 1
Johnson–Cook parameters for the AISI 420 steel material.

$A(MPa)$	$B(MPa)$	C	N	M	$T_r(^\circ C)$	$T_m(^\circ C)$	$\dot{\varepsilon}_0$
450	738	0.02	0.388	0.8	27	1454	1

Table 2
Physical and mechanical parameters for the AISI 420 steel material.

Density(g/cm^3)	Poisson's ratio	Young's Modulus(GPa)	Thermal Conductivity($W/m\ K$)	Specific heat ($J/kg\ ^\circ C$)	Thermal expansion ($10^{-6}\ ^\circ C$)
7.8	0.3	200	24.9	460	10.3

2.3 Shot stream simulation

All of the mentioned shots were perpendicular to the surface. The following basic parameters were similarly assigned to the whole shots: velocity in *Vy* direction, diameter (*D*), the friction between the body surface and shots using the Columbian friction model (Eq. (5)):

$$F_f = \mu F_n \tag{5}$$

Here, F_f is the friction force, μ is the friction coefficient and F_n is the normal force. The μ was chosen as 0.2 for the contact between the shots and the body surface, since for a μ larger than 0.2 the results will not change much [40, 41]. The number of shots is associated with the shot size, the coverage percentage, and the level of impact. In case the shots hit the target successively, the time required for simulation is $N\Delta t$, where *N* is the number of shots and Δt is the time interval in the impacts; however, in case a number of shots simultaneously hit the target surface, the whole simulation time is decreased. For this reason, several rows are assumed for the shots, each of which spaced from the surface proportional to the impact time. The origin of the coordinates is placed in the middle of the body surface so that the *y*-axis is vertical to the surface. The position of the shots in $x-z$ plane varied randomly from one row to another to generate a random impact condition. Therefore, the total time needed for simulation is only $N_y\Delta t$, where N_y is the number of shots rows that is less than *N* in accordance with the number of shots per plane. The modeling phases were as following:

1) A local coordinate system is located at the middle of the body surface, so that the *y*-axis remains perpendicular to the surface.
2) By using the random function, the center coordinates *j-th* shot ($j \geq 1$) is generated in *k-th* row:

$$\begin{aligned} &x_{kj}=random.uniform(-d,d) \\ &z_{kj}=random.uniform(-d,d), \qquad j=1,\ldots N_s,\ k=1,\ldots N_y \\ &y_{kj}=(k-1)V\Delta t+d/2 \end{aligned} \tag{6}$$

where, N_s is the number of shots for each row, and N_y is the number of rows of shots $\left(N_y = N/N_s\right)$ $random.uniform(-d,d)$ is a random number created in the range $(-d,d)$ uniformly, Δt is the time interval between the successive shot hits, which is $3.5\times10^{-6}\,s$ for our model, and *d* is the shot diameter.

3) The distance between the center of the *i-th* shot and the center of the *j-th* shot $(i = 1 \ldots j-1)$ determined through Eq. (7).

$$d_{i,j} = \sqrt{(x_j - x_i)^2 + (z_j - z_i)^2} \quad (7)$$

In case $d_{i,j} < d$, the shot *j* overlaps with the previous shot *i*, which is not possible physically. The shot *j* ought to be removed and return to step 2.

4) Go to step 2 to create the next shot until the creation of the whole shots is finished.

2.4 Shot-peening coverage

The shot-peening coverage is the proportion of the shot area to the total surface area. In statistical sense, the coverage of 100% is obtained only when the target shot-peening is continued for an infinite time, whilst this overlap does not affect the coverage. Generally, coverage of 98% is roughly considered as 100%, and the coverage of 200% is described as twice as long as required to reach 100% [1]. Apparently, the shot-peening coverage has been generated on the basis of the dimple dimensions and the shot-peening time. One can use the Avrami equation to assess the coverage [42]:

$$C = 100\% \times \left(1 - e^{-\pi r^2 Rt}\right) \quad (8)$$

where, *C* is the coverage, *r* indicates the mean dimple radius, and *R* is the number of shot hits in one second for the surface unit, *t* denotes the duration of shot-peening time. Obviously, Rt indicates the whole number of shots for the surface unit. The number of shots was obtained by the Avrami equation. First, the impact of a shot was modeled and its effect was selected as the value of the dimple. The number of rows was selected optionally so that it was logical and proportional with the size of the model. By dividing the number of shots to the number of rows, the number of shots per row was obtained.

3 OPTIMIZATION APPROACH

3.1 Taguchi method

The Taguchi technique is a potent tool in the design of experiment (*DoE*) that is established by *G* Taguchi. In this technique, process optimization engineering should be done in three steps: 1) system design, 2) parameter design, and 3) tolerance design. In the first step, a sample designs is produced. This sample design involves the product design phase and the process design phase. In the second step, the process parameters are optimized. At this point, the best sets for the control parameters are selected. Finally, in the third step, the tolerance around the optimum point is calculated and analyzed. Parametric design is an important step in the Taguchi technique to obtain better results without increasing the cost. Orthogonal arrays are used in the Taguchi method to study the parameter space with a lower number of data. Statistical analysis of variance (ANOVA) is used to identify important parameters. Therefore, the best parameters will be obtained based on the above analysis [43]. Implementation, The *L*9 orthogonal array is used for selecting the parameters required for the simulations, and the results are examined using Minitab18. In this study, three parameters and their importance have been investigated. The parameters are the size of the shot, the velocity of the shot, and the coverage. Each factor is examined at three various levels. Their corresponding levels in real and coded values are presented in Table 3. Finite element analysis is performed for each case and the results of the simulation are presented in Table 4. The desired responses are surface stress, maximum compressive stress, maximum compressive depth, compressive depth, and roughness (*Ra*).

The residual stresses included the residual stresses of the target surface (σ_{surf}^{RS}) and the maximum induced residual stresses (σ_{max}^{RS}). Furthermore, the depths of the maximum residual stress (δ_{max}^{RS}) and the compressive stress depth (δ_{c}^{RS}) are also considered in this study. For estimating the residual stress distribution, the average residual stress is calculated at each depth [44]:

$$\bar{\sigma}_{xx} = \frac{1}{N}\sum_{i=1}^{N}\sigma_{xx}(i) \tag{9}$$

where $\bar{\sigma}_{xx}$ is the averaged stress of σ_{xx}, and N is the number of the stress nodal in its depth. Surface treatment of shot-peening is usually done for increasing the strength of mechanical components of the metal. However, in many cases, there is the possibility of failure or alteration of the shot peened surface by surface defects such as surface roughness [2, 3], which can significantly reduce the fatigue strength [45, 46]. Roughness is defined as a sequence of cavities due to shot-peening. *Ra* is one of the general parameters for measuring the roughness. *Ra* is calculated as the arithmetical mean deviation of the profile [46]:

$$Ra = \frac{1}{l}\int_0^l |Y(x)|dx \tag{10}$$

where $Y(x)$ denotes the peak heights in the sampling length l. The data we get from Gaussian filtering steps describe the surface irregularity without considering the wave component. The displacement of the surface body in the midline was picked as data. The MATLAB code is written to calculate the parameter *Ra* according to their standard definitions.

Table 3
Input factors and their levels.

Parameter	Notation	Level		
		1	2	3
Shot velocity (*m/s*)	*V*	70	90	110
Shot size	*D*	S230(0.5842*mm*)	S280(0.7112*mm*)	S330(0.8282*mm*)
Peening coverage (%)	*C*	100	150	200

Table 4
Taguchi *L*9 array based on parameters levels.

V	*D*	*C*	*R*1: surface stress (*MPa*)	*R*2: max compressive stress (*MPa*)	*R*3: max compressive stress depth (*mm*)	*R*4: depth of compressive stress layer (*mm*)	*R*5: *Ra* (μm)
1	1	1	-657.049	-884.24	0.0623173	0.464302	3.37716
1	2	2	-742.284	-989.01	0.0718268	0.573241	3.10003
1	3	3	-779.417	-1089.36	0.0903453	0.695694	3.12375
2	1	2	-711.953	-984.21	0.0768318	0.558727	3.43826
2	2	3	-769.557	-1079.30	0.0829630	0.719970	3.49841
2	3	1	-724.755	-975.42	0.0830881	0.774775	3.44740
3	1	3	-748.441	-1076.68	0.0868418	0.680178	3.59197
3	2	1	-623.772	-922.10	0.0948498	0.761261	4.13560
3	3	2	-694.396	-1004.27	0.0930981	0.981982	3.63470

3.2 Desirability function approach

The desirability function approach is a common method to optimize the multiple responses simultaneously. In this method, a multi-response problem is converted to a single response using mathematical transformations. In the desirability function approach, the aim is to find the values of the input factors so that all responses have desirability greater than zero and the overall desirability is maximal. Switch and Deringer [47] introduce a proper form of desirability functions that gives a score to each response and sets the input parameters to maximize the total score. To define desirability function approach, each of the n response variables is assumed to depend on k independent input variable through Eq. (11):

$$y_i = f_i(x_1, x_2, \ldots, x_k) + \varepsilon_i \qquad i = 1,2,\ldots,n \tag{11}$$

Here, y_i, is the *i-th* variable of response, f_i is the relationship between this and the input variables (here shot-peening parameters) and ε_i is the error. In desirability function *d*, a value between 0 and 1 is assigned to each response variable y_i . The value 1 shows that the response variable is at the ideal endpoint (target) and 0 shows the worst case of desirability for the response variable. Optimization of the corresponding response cause to increase in the value of *d*. Depending on the purpose of maximizing, minimizing, or reaching a specific value, various desirability functions can be defined. If a response is of the "target is best" type, then the desirability function is:

$$d_i = \begin{cases} 0 & \text{if } y_i \le L_i \\ \left(\dfrac{y_i - L_i}{T_i - L_i}\right)^{r_i} & \text{if } L_i < y_i < T_i \\ \left(\dfrac{y_i - U_i}{T_i - U_i}\right)^{t_i} & \text{if } T_i < y_i < U_i \\ 0 & \text{if } y_i \ge U_i \end{cases} \tag{12}$$

If the goal is to maximize the desirability function:

$$d_i = \begin{cases} 0 & \text{if } y_i \le L_i \\ \left(\dfrac{y_i - L_i}{T_i - L_i}\right)^{r_i} & \text{if } L_i < y_i < T_i \\ 1 & \text{if } y_i \ge T_i \end{cases} \tag{13}$$

In the case of minimizing the target:

$$d_i = \begin{cases} 1 & \text{if } y_i \le T_i \\ \left(\dfrac{y_i - U_i}{T_i - U_i}\right)^{r_i} & \text{if } T_i < y_i < U_i \\ 0 & \text{if } y_i \ge U_i \end{cases} \tag{14}$$

L_i , U_i and T_i are the lower, upper and target value respectively and r_i , t_i coefficient is set by the user and define the importance of hitting the target value. If $r_i = 1$, then the desirability function increases linearly. For $r_i < 1$, the desirability function is convex and concave for $r_i > 1$. Generally, r_i and t_i is considered one. In the maximum case, T_i is selected a large enough value for the response. In the minimum case, T_i indicating a small enough value for the response. After the desirability values for each response variable are determined, they are mixed in the form of the unit desirability function, which this final desirability function is calculated in Eq. (14):

$$D = \left(\prod_{i=1}^{n} d_i\right)^{\frac{1}{n}} \tag{15}$$

Here, *D* is the final desirability function, d_i is the individual desirability function of each response variable, and *n* is the number of response variables. Now *D* must be maximized.

3.3 The proposed hybrid approach

Given the advantages of the Taguchi method and the desirability function method, these two methods can be combined to reduce their's limitations. For this purpose, all the responses can be converted to values between 0 and 1 with the desirability functions (Eqs. (12-14)). Then, using the Taguchi method, the final desirability function is optimized and its maximum value is obtained. For shot-peening problem, optimization process is rewritten as follows:

function	desired mode
$R1: \sigma_{surf}^{RS}$	*min*
$R2: \sigma_{max}^{RS}$	*min*
$R3: \delta_{max}^{RS}$	*max*
$R4: \delta_{c}^{RS}$	*max*
$R5: Ra$	*min*

To multi-objective optimization, one can select two, three, or all of the above functions. The target value T_i can be considered from the single-objective optimization with the traditional Taguchi method.

4 RESULTS AND DISCUSSION

4.1 Effective parameters

Table 5-9 show the ANOVA table for this study. The "*F*-test" can be used to specify which process parameters factors have a significant influence on the quality characteristic. The value of *F* can also be used to rank factors. According to Table 5, it is concluded that the effective parameters for surface stress are *C, V*, and *D*, respectively. Coverage *C* has the highest impact. According to Table 6, the effective parameters for maximum compressive stress are *C, D*, and *V*, respectively. Again, coverage *C* is most affected. According to Table 7, for the depth of the maximum compressive stress, the effective parameters are *V, D*, and *C*, respectively. According to Table 8, the effective parameters for compressive stress depth are *D, V*, and *C*, respectively. Similar to the previous section, the results of the ANOVA analysis for roughness *Ra* are presented in Table 9. By examining the *F*-test for different terms, it is concluded that the effective parameter is *V* and then *C* and *D*, respectively.

Table 5
Analysis of variance for means *R*1.

Source	DF	Seq SS	Adj SS	Adj MS	*F*	*P*
V	2	3648	3648	1824.2	1.73	0.367
D	2	1208	1208	604.2	0.57	0.636
C	2	14197	14197	7098.4	6.71	0.130
Residual Error	2	2114	2114	1057.1		
Total	8	21168				

Table 6
Analysis of variance for means *R*2.

Source	DF	Seq SS	Adj SS	Adj MS	*F*	*P*
V	2	971.9	971.9	485.9	1.06	0.484
D	2	2621.2	2621.2	1310.6	2.87	0.258
C	2	36107.0	36107.0	18053.5	39.55	0.025
Residual Error	2	913.0	913.0	456.5		
Total	8	40613.1				

Table 7
Analysis of variance for means *R*3.

Source	DF	Seq SS	Adj SS	Adj MS	*F*	*P*
V	2	0.000432	0.000432	0.000216	3.96	0.202
D	2	0.000276	0.000276	0.000138	2.53	0.283
C	2	0.000082	0.000082	0.000041	0.75	0.571
Residual Error	2	0.000109	0.000109	0.000055		
Total	8	0.000899				

Table 8
Analysis of variance for means *R*4.

Source	DF	Seq SS	Adj SS	Adj MS	*F*	*P*
V	2	0.079530	0.079530	0.039765	17.09	0.055
D	2	0.093682	0.093682	0.046841	20.13	0.047
C	2	0.002484	0.002484	0.001242	0.53	0.652
Residual Error	2	0.004654	0.004654	0.002327		
Total	8	0.180350				

Table 9
Analysis of variance for means *Ra*.

Source	DF	Seq SS	Adj SS	Adj MS	*F*	*P*
V	2	0.51916	0.51916	0.25958	9.65	0.094
D	2	0.04737	0.04737	0.02368	0.88	0.532
C	2	0.13088	0.13088	0.06544	2.43	0.291
Residual Error	2	0.05380	0.05380	0.02690		
Total	8	0.75121				

The effect of each shot-peening parameter could be represented by the response graph. These graphs show the response change when the parameters change their level from 1 to 3. Fig. 2 shows the significant effect of input factors on the surface stress. It can be seen graphically from Fig. 2 that parameter *C* has the highest notable effect. The shot velocity has a nonlinear effect on the surface stress, with its highest intensity being at level 2 (90 *m/s*). On the other hand, the results show that the surface stress increases with increasing coverage and shot size.

The same results can be seen for maximum compressive stress from Fig. 3 and show the same trend. However, the effect of velocity on surface stress is more evident.

Figs. 4 and 5 show the effect of parameters on the depth of the maximum compressive stress and the compressive stress depth. The two diagrams are similar and show the same trend. It can be seen that *V* and *D* have a great effect on the depths and *C* is less effective.

Fig. 6 shows the main effect of input factors on the roughness produced by the shot-peening. It can be concluded that the shot velocity is more effective than other parameters. Shot diameter *D* has a nonlinear effect and effect of *C* is low. It is obvious from the results that *C* and *V* simultaneously do not have a leading effect on the responses, and depending on the response, one of them (not both) has a dominant effect.

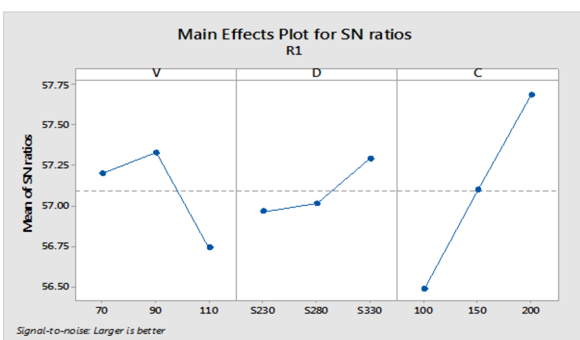

Fig.2
Mean *S/N* ratio vs inputs for *R*1 (surface stress).

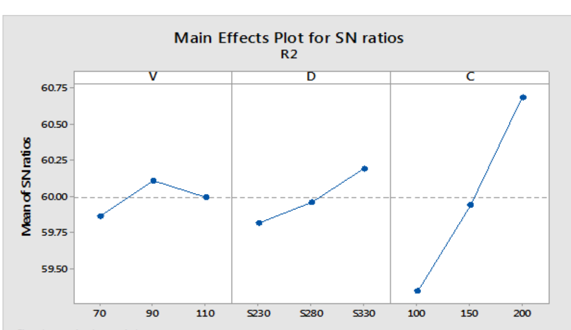

Fig.3
Mean *S/N* ratio vs inputs for *R*2 (max compressible stress).

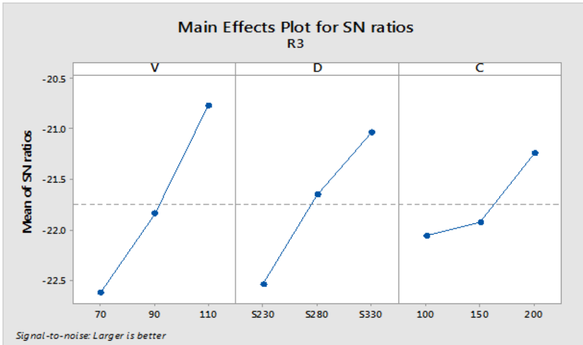

Fig.4
Mean S/N ratio vs inputs for $R3$ (the depth of the maximum compressible stress).

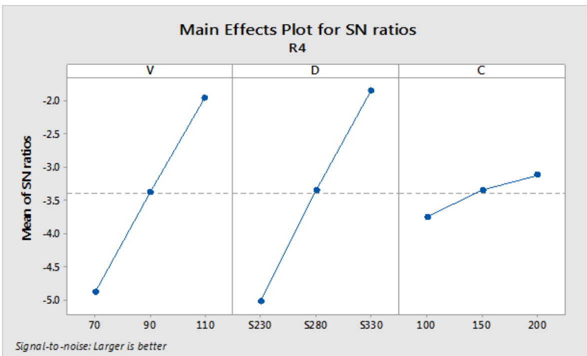

Fig.5
Mean S/N ratio vs inputs for $R4$ (compressible stress depth).

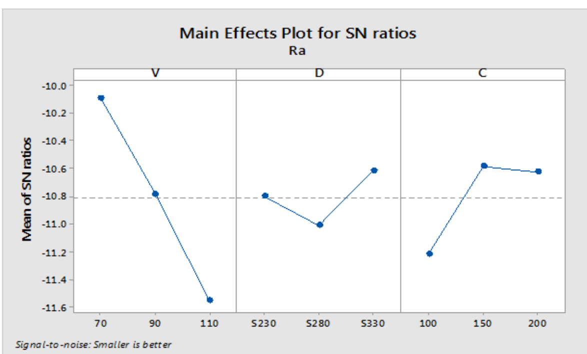

Fig.6
Mean S/N ratio vs inputs for Ra.

4.2 Optimization of shot-peening parameter

Optimal levels can be easily selected using Figs. 2-6. For the optimal value of each response, it is enough to individually select any parameter that gives the higher S/N ratio. For example, in surface stress, the optimum levels of V, D, and C are levels 2, 3, and 3, respectively, because the S/N ratio is higher in these levels. Table 10 gives the settings of the levels to get the optimal value of different responses. The optimum parameters for the stresses are the same and for the depths of the stresses are identical too.

Note that the optimal values obtained in Table 10 are considered as single-objective, so the optimal values for each quantity can refuse to be the optimal point for other quantities. Such a situation is not desirable because the increase in the fatigue life of the dependent part is simultaneously the compressive residual stress and roughness, and if only one of the responses is optimal, fatigue life may not improve or even decrease. Thus, it is important to optimize simultaneous responses in multi-objective optimizations.

For the sake of comparison, optimum parameters are determined based on the proposed method and the method presented in [48], and depicted in Table 11. As can be seen, obtained parameters are approximately equal to parameters, presented in [48], and differences between responses are maximally up to 5.3 percent, which corresponds to Taguchi method prediction. The superiority of proposed method is the very lower expense in calculation process but in responses, there are minimum differences between them. Using the procedure described above, we can find the optimal parameters for single-objective functions only. Converting the values of Table 4 to their desirability values are given in Table 12 for the various single and multiple functions. Since the values of Table 4, undergo linear conversion, so to find optimum parameters for the single-objective functions using these values and the Taguchi method, we reach at the same results in Table 10. Now we can find optimal values for multi-objective functions.

Figs. 7-10 show the effects of the input parameters on the desirability of the two responses simultaneously.

Table 10
Optimal shot-peening parameters for different target functions.

	Objective function	Optimum parameter			Optimum value
		V(m/s)	*D*	*C(%)*	
1	*R*1	90	S330(0.8383*mm*)	200	-800.39 *MPa*
2	*R* 2	90	S330(0.8383*mm*)	200	-1116.75 *MPa*
3	*R* 3	110	S330(0.8383*mm*)	200	0.102 *mm*
4	*R* 4	110	S330(0.8383*mm*)	200	0.984 *mm*
5	*Ra*	70	S330(0.8383*mm*)	150	3.027 *μm*

Table 11
Optimal shot-peening parameters for different target functions from reference [48].

	Objective function	Optimum parameter [48]			Optimum value	difference
		V(m/s)	*D(mm)*	*C(%)*		
1	*R*1	-	-	200	-760.18 *MPa*	5.3%
2	*R* 2	-	0.8382	200	-1101.93 *MPa*	1.3%
3	*R* 3	110	0.8382	-	0.099 *mm*	3.0%
4	*R* 4	110	0.8382	200	1 *mm*	1.6%
5	*Ra*	70	-	-	3.1 *μm*	2.4%

Table 12
Taguchi *L*9 array based on parameters levels.

V	*D*	*C*	*R*1	*R*2	*R*3	*R*4	*Ra*	*R*1 & *Ra*	*R*2 & *Ra*	*R*3 & *Ra*	*R*4 & *Ra*	*R*1 & *R* 3 & *Ra*	*R* 1 & *R* 2 & *R* 3 & *R* 4 & *Ra*
1	1	1	0.188	0.000	0.000	0.000	0.684	0.359	0.000	0.000	0.000	0.000	0.000
1	2	2	0.671	0.451	0.240	0.210	0.934	0.792	0.649	0.473	0.443	0.532	0.427
1	3	3	0.881	0.882	0.706	0.445	0.913	0.897	0.897	0.803	0.637	0.828	0.741
2	1	2	0.499	0.430	0.366	0.182	0.629	0.560	0.520	0.480	0.338	0.486	0.390
2	2	3	0.825	0.839	0.520	0.492	0.575	0.689	0.694	0.547	0.532	0.627	0.633
2	3	1	0.572	0.392	0.523	0.597	0.621	0.596	0.493	0.570	0.609	0.571	0.534
3	1	3	0.706	0.828	0.618	0.415	0.490	0.588	0.637	0.551	0.451	0.598	0.593
3	2	1	0.000	0.163	0.820	0.571	0.000	0.000	0.000	0.000	0.000	0.000	0.000
3	3	2	0.400	0.516	0.776	0.996	0.452	0.425	0.483	0.592	0.671	0.519	0.591

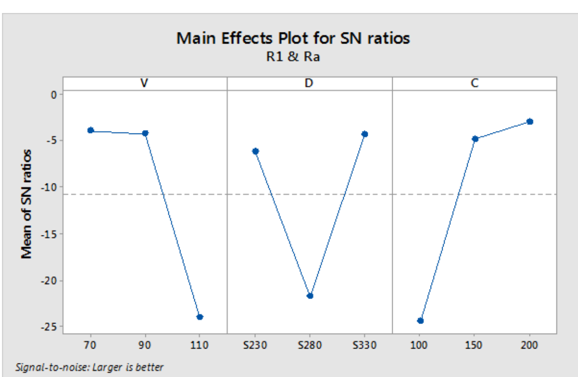

Fig.7
Mean *S/N* ratio vs inputs for desirability function of *R*1 and *Ra*.

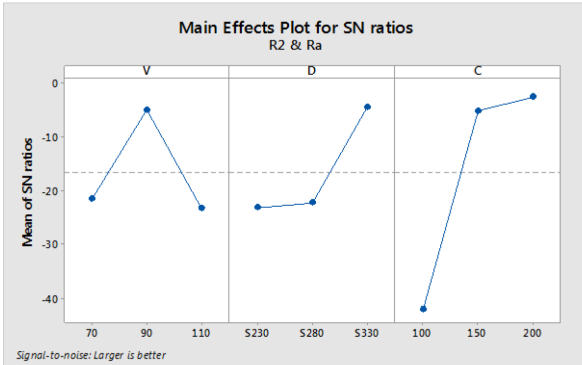

Fig.8
Mean *S/N* ratio vs inputs for desirability function of *R*2 and *Ra*.

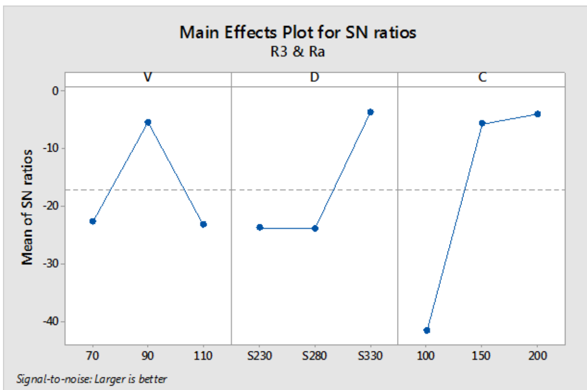

Fig.9
Mean *S/N* ratio vs inputs for desirability function of *R*3 and *Ra*.

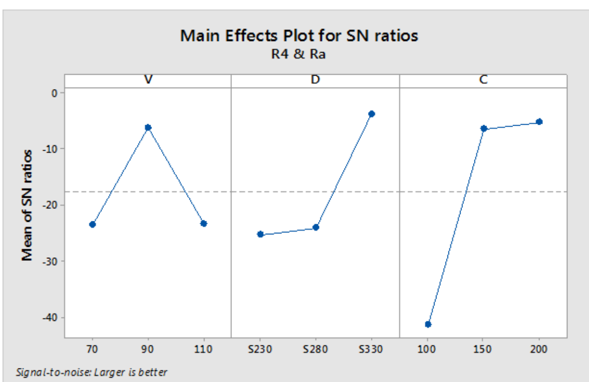

Fig.10
Mean *S/N* ratio vs inputs for desirability function of *R*4 and *Ra*.

Fig. 11 and 12 illustrate the desirability for the three and five responses simultaneously. Using these graphs, we can easily and quickly estimate the optimal parameters for multi-objective functions. The results are shown in Table 13. It is seen from Table 13 that the optimal parameters for simultaneous optimization of surface compressive stress and *Ra* are obtained with high *C*, high shot diameter and low shot velocity. The reason is that most important parameter of the surface stress is the coverage of *C*, whereas for *Ra* is the velocity, so with high *C* and low velocity we can achieve optimal point. In other case, high *C* and medium shot velocity are selected. With high *C*, high shot diameter and low shot velocity all of responses are optimized.

In order to compare the optimum parameters are determined based on the proposed method and the method presented in [48], and depicted in Table 14. It can be seen that the obtained parameters in this paper are the same results presented in [48], except the simultaneous optimization of *R*2 and *Ra* in which the velocity is different while the maximum difference in stress responses is 6.5 percent. In other cases, differences between responses, is lower than this amount which is related to the difference between computational and predicted models. Therefore, the proposed method has some advantages such as lower computational cost and simple application for multi variable problems.

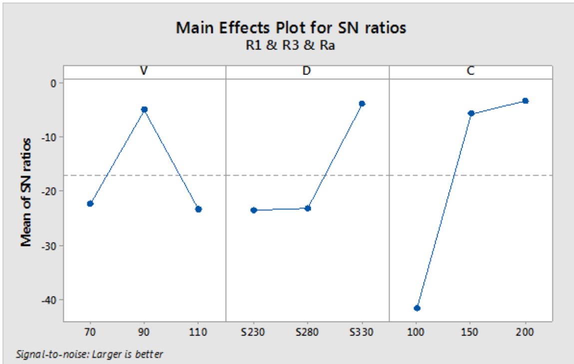

Fig.11
Mean *S/N* ratio vs inputs for desirability function of *R*1, *R*3 and *Ra*.

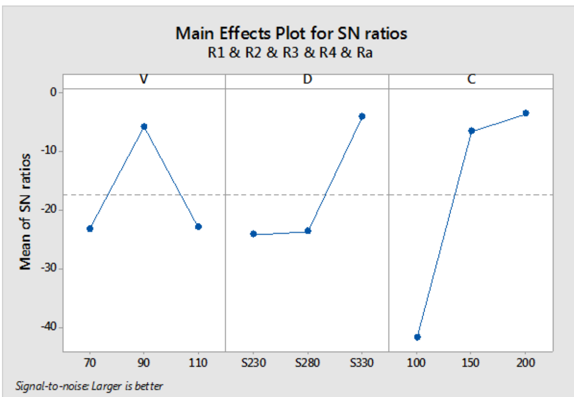

Fig.12
Mean *S/N* ratio vs inputs for desirability function of all responses.

Table 13
Optimal shot-peening parameters for multiple target functions.

	Objective functions	Optimum parameter			Opt. value
		V(*m/s*)	*D*	*C*(%)	
1	*R*1 & *Ra*	70	S330(0.8382*mm*)	200	-790.51 *MPa* & 3.16 *μm*
2	*R*2 & *Ra*	90	S330(0.8382*mm*)	200	-1116.75 *MPa* & 3.302 *μm*
3	*R*3 & *Ra*	90	S330(0.8382*mm*)	200	0.0916 *mm* & 3.302 *μm*
4	*R*4 & *Ra*	90	S330(0.8382*mm*)	200	0.821 *mm* & 3.302 *μm*
5	*R*1 & *R*3 & *Ra*	90	S330(0.8382*mm*)	200	-800.39 *MPa* & 0.0916 *mm* & 3.302 *μm*
6	*R*1 & *R*2 & *R*3 & *R*4 & *Ra*	90	S330(0.8382*mm*)	200	-800.39 *MPa* & -1116.75 *MPa* & 0.0916 *mm* & 0.821 *mm* & 3.302 *μm*

Table 14
Optimal shot-peening parameters for multiple target functions from reference [48].

	Objective functions	Optimum parameter [48]			Opt. value	Difference
		V(*m/s*)	*D*(*mm*)	*C*(%)		
1	*R*1 & *Ra*	70	-	200	-760.18 *MPa* & 3.1 *μm*	4.0% & 1.9%
2	*R*2 & *Ra*	70	0.8382	200	-1101.93 *MPa* & 3.1 *μm*	1.3% & 6.5%
6	*R*1 & *R*2 & *R*3 & *R*4 & *Ra*	90.12	0.8382	200	-760.18 & -1101.93 & 0.088 & 0.85 & 3.43	5.3% & 1.3% & 4.1% & 3.4% & 3.7%

4.3 Validation of the simulation

In this section, the models obtained from the results section are validated and compared with the experimental data. The operating conditions are as:

(i) Shot *S*170, (ii) Intensity Almen 14*A*, (equivalent to velocity 67.7 *m/s*), (iii) Coverage 100%, (iv) Impact angles 90 degree.

The coefficient of friction μ between the shots and the surface is 0.2.

Fig. 13 shows the comparison between the experimental results and the residual compressive stress profile obtained numerically. A satisfactory correspondence is observed between the calculated results and experimental values. Fig. 14 shows the contour of the stress S11.

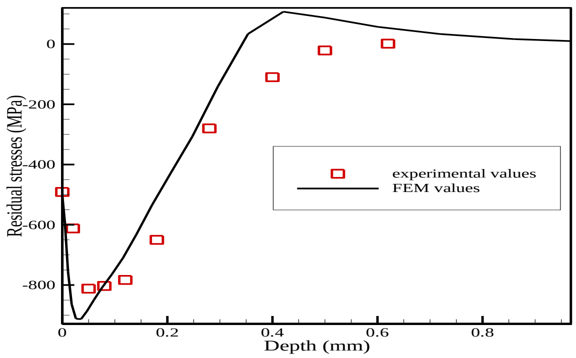

Fig.13
Residual-stress profiles in-depth of shot-peened AISI 420.

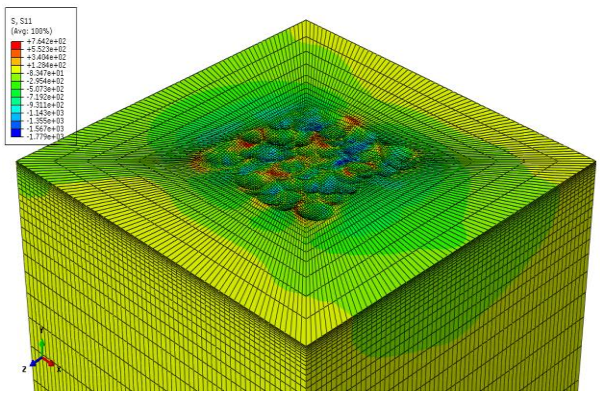

Fig.14
Stress contour (S11) of shot peened surface.

4.4 Confirmation test

To ensure the reproduction of the combination of parameters obtained from finite element results, a verification test is performed under the optimal parameters of shot-peening (shot velocity, shot size, and coverage)-(70 *m/s*, S330 *mm* and 200%). Residual surface stress is -769.65 *MPa* and the *Ra* is 3.04 *µm*.

5 CONCLUSIONS

The paper presented suitable and reliable methods to optimize the response variables (residual stress and surface roughness) simultaneously to determine the optimal parameters of the shot-peening process by minimum numerical cost. The main results are as follows:

1. By simulating the shot-peening process and using Taguchi approach, it was clarified that:
   - The most important parameter for the surface residual stress and the maximum residual stress is the coverage *C*.
   - The depth of maximum compressive stress and the depth of compressive stress layer are directly related to the velocity and diameter of the shot.
   - Roughness is highly dependent on the shot velocity.
2. As one of the common applications of shot-peening is to increase fatigue life, simultaneous attention to inductive compressive stress and roughness caused by shot-peening is important. Therefore, multi-objective optimization methods are recommended.
3. With high-coverage and low-velocity, one can reach optimal conditions for surface stress and roughness (*Ra*) simultaneously.

4. The proposed method has a proper and reliable performance in determining the optimal parameters in a multi-objective way and it can quickly and easily find the optimal parameters.

REFERENCES

[1] S.A.E. Handbook, 1986, *Society of Automotive Engineers*, SAE Publications.

[2] Fathallah R., Sidhom H., Braham C., Castex L., 2003, Effect of surface properties on high cycle fatigue behaviour of shot peened ductile steel, *Materials Science and Technology* **19**: 1050-1056.

[3] Eleiche A., Megahed M., Abd-Allah N., 2001,The shot-peening effect on the HCF behavior of high-strength martensitic steels, *Journal of Materials Processing Technology* **113**: 502-508.

[4] Hills D., Waterhouse R., Noble B., 1983, An analysis of shot-peening, *The Journal of Strain Analysis for Engineering Design* **18**: 95-100.

[5] Al-Obaid Y., 1995, Shot-peening mechanics: experimental and theoretical analysis, *Mechanics of Materials* **19**: 251-260.

[6] Obata M., Sudo A., 1993, Effect of shot-peening on residual stress and stress corrosion cracking for cold worked austenitic stainless steel, *Proceedings of the ICSP-5 Conference*, Oxford, UK.

[7] Dorr T., Hilpert M., Beckmerhagen P., Kiefer A., Wagner L., 1999, Influence of shot-peening on fatigue performance of high-strength aluminum-and magnesium alloys, *7th ICSP American Shot-peening Society*.

[8] Hong T., Ooi J., Shaw B., 2008, A numerical simulation to relate the shot-peening parameters to the induced residual stresses, *Engineering Failure Analysis* **15**: 1097-1110.

[9] Meguid S., Shagal G., Stranart J., Daly J., 1999, Three-dimensional dynamic finite element analysis of shot-peening induced residual stresses, *Finite Elements in Analysis and Design* **31**: 179-191.

[10] Guagliano M., 2001, Relating Almen intensity to residual stresses induced by shot-peening: a numerical approach, *Journal of Materials Processing Technology* **110**: 277-286.

[11] Kim T., Lee J.H., Lee H., Cheong S.-k., 2010, An area-average approach to peening residual stress under multi-impacts using a three-dimensional symmetry-cell finite element model with plastic shots, *Materials & Design* **31**: 50-59.

[12] Ghasemi A., Hassani-Gangaraj S.M., Mahmoudi A., Farrahi G., Guagliano M., 2016, Shot-peening coverage effect on residual stress profile by FE random impact analysis, *Surface Engineering* **32**: 861-870.

[13] Miao H., Larose S., Perron C., Lévesque M., 2009, On the potential applications of a 3D random finite element model for the simulation of shot-peening, *Advances in Engineering Software* **40**: 1023-1038.

[14] Mahmoudi A., Ghasemi A., Farrahi G., Sherafatnia K., 2016, A comprehensive experimental and numerical study on redistribution of residual stresses by shot-peening, *Materials & Design* **90**: 478-487.

[15] Nam Y.-S., Jeon U., Yoon H.-K., Shin B.-C., Byun J.-H., 2016, Use of response surface methodology for shot-peening process optimization of an aircraft structural part, *The International Journal of Advanced Manufacturing Technology* **87**: 2967-2981.

[16] AlSumait A., Li Y., Weaser M., Niji K., Battel G., Toal R., 2019, A Comparison of the Fatigue Life of Shot-Peened 4340M Steel with 100, 200, and 300% Coverage, *Journal of Materials Engineering and Performance* **28**: 1780-1789.

[17] Petit-Renaud F., Evans J., Metcalfe A., Shaw B., 2008, Optimization of a shot-peening process, *Proceedings of the Institution of Mechanical Engineers, Part L: Journal of Materials: Design and Applications* **222**: 277-289.

[18] Romero J.S., Rios E., Fam Y., Levers A., 2002, *Optimisation of the Shot-Peening Process in Terms of Fatigue Resistance*, University of Sheffield.

[19] Vielma A., Llaneza V., Belzunce F., 2014, Shot-peening intensity optimization to increase the fatigue life of a quenched and tempered structural steel, *Procedia Engineering* **74**: 273-278.

[20] Unal O., 2016, Optimization of shot-peening parameters by response surface methodology, *Surface and Coverages Technology* **305**: 99-109.

[21] Bhuvaraghan B., Srinivasan S.M., Maffeo B., Prakash O., 2011, Constrained probabilistic multi-objective optimization of shot-peening process, *Engineering Optimization* **43**: 657-673.

[22] Baragetti S., 1997, Shot-peening optimisation by means of DOE: Numerical simulation and choice of treatment parameters, *International Journal of Materials and Product Technology* **12**: 83-109.

[23] Seddik R., Bahloul A., Atig A., Fathallah R., 2017, A simple methodology to optimize shot-peening process parameters using finite element simulations, *The International Journal of Advanced Manufacturing Technology* **90**: 2345-2361.

[24] Roy R.K., 2001, *Design of Experiments Using the Taguchi Approach*, New York, John Willey & Sons.

[25] George P., Pillai N., Shah N., 2004, Optimization of shot-peening parameters using Taguchi technique, *Journal of Materials Processing Technology* **153**: 925-930.

[26] Khany S.E., 2015, An experimental study of the effect of shot peening on the low carbon steel and identification of optimal process parameters, *Materials Today: Proceedings* **2**(4-5): 3363-3370.

[27] Maleki E., Okan U., Kashyzadeh K.R., 2019, Efficiency analysis of shot peening parameters on variations of hardness, grain size and residual stress via taguchi approach, *Metals and Materials International* **25**(6): 1436-1447.

[28] Shiau G.H., 1990, A study of the sintering properties of iron ores using the Taguchi's parameter design, *Journal of the Chinese Statistical Association* **28**: 253-275.

[29] Tong L.I., Su C.T., Wang C.H., 1997, The optimization of multi-response problems in the Taguchi method, *International Journal of Quality and Reliability Management* **14**(4): 367-380.
[30] Logothetis N., Haigh A., 1988, Characterizing and solving multi-response processes by the Taguchi method, *Quality and Reliability Engineering International* **4**(2): 159-169.
[31] Pignatello J.J.,1993, Strategies for robust multi-response quality engineering, *IIE Transactions* **25**: 5-15.
[32] Tong L.-I., Su C.-T., 1997, Optimizing multi-response problems in the Taguchi method by fuzzy multiple attribute decision making, *Quality and Reliability Engineering International* **13**: 25-34.
[33] Su C.T., Tong L.I., 1997, Multi-response robust design by principal component analysis, *Total Quality Management* **8**(6): 409-416.
[34] Antony J., 2000, Multi-response optimization in industrial experiments using Taguchi's quality loss function and principal component analysis, *Quality and Reliability Engineering International* **16**: 3-8.
[35] Liao H.C., Chen Y.K., 2002, Solving multi-response problem in the Taguchi method by DEA based ranking method, *International Journal of Quality & Reliability Management* **19**(7): 825-837.
[36] Wong Y.H.W., Beasley J.E., 1990, Restricting weight flexibility in DEA, *The Journal of the Operational Research Society* **41**: 829-835.
[37] Baker R.C., Talluri S., 1997, A closer look at the use of data envelopment analysis for technology selection, *Computers and Industrial Engineering* **28**: 101-108.
[38] Kim T., Lee H., Jung S., Lee J.H., 2012, A 3D FE model with plastic shot for evaluation of equi-biaxial peening residual stress due to multi-impacts, *Surface and Coverages Technology* **206**: 3125-3136.
[39] Gangaraj S.M.H., Guagliano M., Farrahi G.H., 2014, An approach to relate shot peening finite element simulation to the actual coverage, *Surface and Coatings Technology* **243**: 39-45.
[40] Kim T., Lee H., Hyun H.C., Jung S., 2013, Effects of rayleigh damping, friction and rate-dependency on 3D residual stress simulation of angled shot peening, *Materials & Design* **46**: 26-37.
[41] Yang F., Yukui G., 2016, Predicting the peen forming effectiveness of Ti-6Al-4V strips with different thicknesses using realistic finite element simulations, *Journal of Engineering Materials and Technology* **138**(1):011004.
[42] Kirk D., 2005, Theoretical principles of shot-peening coverage, *Shot Peener* **19**: 24-28.
[43] Singh L., Khan R.A., Aggarwal M.L., 2013, Multi performance characteristic optimization of shot peening process for AISI 304 austenitic stainless steel using grey relational analysis with principal component analysis and Taguchi method, *American Journal of Engineering Research* **2**(10): 160-172.
[44] Gariépy A., Miao H.Y., Lévesque M., 2017, Simulation of the shot peening process with variable shot diameters and impacting velocities, *Advances in Engineering Software* **114**: 121-133.
[45] Wagner L., 1999, Mechanical surface treatments on titanium, aluminum and magnesium alloys, *Materials Science and Engineering: A* **263**: 210-216.
[46] ISO 4287, 1997, *Geometrical Product Specifications (GPS)–Surface Texture: Profile Method–Terms, Definitions and Surface Texture Parameters*.
[47] Derringer G., Suich R., 1980, Simultaneous optimization of several response variables, *Journal of Quality Technology* **12**: 214-219.
[48] Hassanzadeh M., Moussavi Torshizi S.E., 2020, Multi-objective optimization of shot-peening parameters using design of experiments and finite element simulation: a statistical model, *Journal of Applied and Computational Mechanics*, 10.22055/JACM.2020.33102.2152.